J. Membrane Biol. 101, 209–223 (1988)

The Journal of
Membrane Biology

Development of the Fast Sodium Current in Early Embryonic Chick Heart Cells

Shiroh Fujii*, Richard K. Ayer, Jr.,** and Robert L. DeHaan†
Department of Anatomy and Cell Biology†, Emory University Health Science Center, Atlanta, Georgia 30322

Summary. Single ventricle cells were dissociated from the hearts of two-, three-, four-, or seven-day-old chick embryos, and were maintained in vitro for an additional 6 to 28 hr. Rounded 13 to 18 μm cells with input capacitance of 5 to 10 pF were selected for analysis of fast sodium current (I_{Na}). Voltage command protocols designed to investigate the magnitude, voltage dependence, and kinetics of I_{Na} were applied with patch electrodes in the whole-cell clamp configuration. I_{Na} was present in over half of the 2d, and all 3d, 4d and 7d cells selected. The current showed no systematic differences in activation kinetics, voltage dependence, or tetrodotoxin (TTX) sensitivity with age or culture conditions. Between the 2d and 7d stages, the rate of current inactivation doubled and channel density increased about eightfold. At all stages tested, I_{Na} was blocked by TTX at a half-effective concentration of 0.5 to 1.0 nM. We conclude that the lack of Na dependence of the action potential upstroke on the second day of development results from the relatively depolarized level of the diastolic potential, and failure to activate the small available excitatory Na current. The change from Ca to Na dependence of the upstroke during the third to the seventh day of incubation results partly from the negative shift of the diastolic potential during this period, and in part from the increase in available Na conductance.

Key Words sodium current · embryonic heart · tetrodotoxin · membrane channels · patch clamp

Introduction

The sharp upstroke of the cardiac action potential (AP) is carried by a rapid influx of sodium ions termed the "excitatory sodium current" (I_{Na}) (Draper & Weidmann, 1951; Colatsky, 1980; Fozzard, January & Makielski, 1985). I_{Na} has been recorded from isolated cardiac cells (Brown, Lee & Powell, 1981), and single sodium channel currents have been measured in membrane patches from a variety of cardiac preparations (for reviews *see* Cachelin et al., 1983; Reuter, 1984; Makielski et al., 1987). The sodium channel macromolecule has been isolated and reconstituted in a functional state in planar phospholipid bilayers (Keller et al., 1986), and active channels have been expressed in *Xenopus* oocytes after injection with chick muscle mRNA (Sigel, 1987). Moreover, the complete primary amino-acid sequence of the channel protein from eel electroplax has been deduced from its cDNA sequence (Noda et al., 1984, 1986). Nonetheless, we know little about how these macromolecules are expressed during embryogenesis, or even when sodium channels first appear and begin to function in normal cardiac development. In the chick heart, for example, the AP's that characterize the tissue early on the second day of incubation are different than they will be a few days later in development, in size and shape (Fujii, Hirota & Kamino, 1981), and in their responses to pharmacological and ionic perturbations (for review *see* DeHaan, 1980; Marcus & Fozzard, 1981). Ventricular tissue from embryos aged 2 to 3 days fires AP's that arise from a maximal diastolic potential of −50 to −60 mV and have slow rise-times (5 to 30 V/sec). TTX fails to suppress spontaneous activity even at high (micromolar) concentrations (Shigenobu & Sperelakis, 1971; McDonald, Sachs & DeHaan, 1972; Marcus & Fozzard, 1981) and this toxin was been reported to cause little (Ishima, 1968; Iijima & Pappano, 1979) or no (Sperelakis & Shigenobu, 1972; DeHaan, McDonald & Sachs, 1975) reduction in upstroke velocity. In contrast, ventricular tissue taken from the heart after seven days of development or later, has AP's with maximal diastolic potentials of about −90 mV (Nathan, Pooler & DeHaan, 1976; Veenstra & DeHaan, 1986). The rising phase of the AP has a maximal upstroke velocity ($\dot{V}_{max}$) of 150 to 200 V/sec, and is suppressed by nanomolar TTX (DeHaan, 1980; Marcus & Fozzard, 1981).

The slow upstroke of the cardiac AP at two to

* *Present Address:* Department of Biological Sciences and Technology, Science University of Tokyo; Oshamanbe, Yamakoshi-gun, Hokkaido 049-35, Japan.

** *Present Address:* Department of Biology, Yale University, New Haven, Connecticut 06510.

three days of development and its insensitivity to TTX suggest that I_{Na} makes little or no contribution at these early stages. Functional sodium channels may be lacking, or if present in the cardiac cell membrane, the relatively depolarized diastolic potential fails to activate them. To distinguish between these alternatives, Sperelakis and Shigenobu (1972) attempted to increase the maximal upstroke velocity of 3-day heart cells with hyperpolarizing current-clamp pulses, but were unable to do so. They concluded that the fast sodium channel system was absent from young hearts. With the two-electrode voltage-clamp method, Nathan and DeHaan (1978) and Ebihara et al. (1980), recorded excitatory sodium current from clusters of embryonic ventricle cells from hearts during the second week of development, but no similar analysis has been applied to earlier preparations.

In contrast to the findings above, there is a body of evidence suggesting that the embryonic cardiac membrane possesses sodium channels prior to seven days of development. Ishima (1968) reported that TTX (1 μM) and low-sodium solutions affect the 3d AP, and Galper and Catterall (1978) demonstrated that veratridine causes a threefold increase in a TTX-sensitive current in monolayers of 3d ventricular cells. Furthermore, homogenates of 3d heart contain binding sites for a radiolabeled derivative of TTX, [^{3}H]en-TTX (Lombet et al., 1981), and 3d ventricle-cell aggregates after two days in culture are responsive to sea anemone toxin and batrachotoxin (Lazdunski et al., 1982).

To determine the time of appearance of the fast sodium conductance mechanism, and to explore its properties and rate of increase during early cardiac development, we have applied the whole-cell recording patch-electrode technique to single ventricle cells isolated from 2d to 7d hearts. Preliminary results indicated that a fully functional, voltage-activated TTX-sensitive I_{Na} current is present in the 2d (stage 12) heart cell, and that current amplitude increased sharply during the first week of development (Fujii, Ayer & DeHaan, 1986*a*). In the present work, we have explored further the kinetics and TTX-sensitivity of the early sodium current, and have compared its properties to those of I_{Na} at later stages.

Materials and Methods

Cell Preparation

White Leghorn chick embryos were harvested at stage 12 (2d), or after three, four or seven days of incubation at 37.5°C. Cells were isolated by a multiple-cycle dissociation procedure (McDonald & DeHaan, 1973; Nathan & DeHaan, 1979) using trypsin or collagenase. The cell suspensions from 4d and 7d ventricle were transferred to plastic tissue culture dishes (type 3001, Falcon Plastics) for 1 hr to allow fibroblasts to adhere and enrich the supernatant suspension for myocytes. Ventricles from 2d or 3d hearts were dissected and dissociated individually under microscopic observation. Since hearts at these early stages contain relatively few fibroblasts (Manasek, 1970), the myocyte enrichment procedure was not required. The cells were resuspended in tissue culture medium (M21212) and transferred to nonadhesive plastic petri dishes (type 1008, Falcon Plastics), coated with polylysine (0.1 mg/ml), or treated with concentrated sulfuric acid to increase their adhesiveness slightly. In an atmosphere of 5% CO_2, 10% O_2, 85% N_2, the cells attached without appreciable flattening during incubation for 5 to 24 hr.

In a few cases it was possible to free intact isolated cells from 2d ventricle by mechanical maceration in low-Ca phosphate-buffered balanced salt solution without enzyme digestion. The measurements made 6 to 8 hr after dissociation were on cells prepared by this enzyme-free procedure. At all stages, single spherical cells 13 to 18 μm in diameter were selected for experiments. Since physiological differentiation is known to continue in cardiac cells in vitro (Nathan & DeHaan, 1978), we have referred to these preparations by their total actual developmental age, for example, 2d + 8h, or 4d + 1, meaning cells taken from the heart of a 2d (two-day) embryo and maintained in vitro for 8 hr, or from 4d heart, cultured for one additional day.

Scanning Electron Microscopy

After dissociation in a solution containing crystalline trypsin, cells were washed in medium 21212 and incubated for 24 hr in vitro in a humidified gassed atmosphere of 85% N_2, 10% O_2, and 5% CO_2. Cells adhering to a chip of polylysine-coated plastic (Thermonox) were washed five times in 37°C BSS containing (in mM): 142 NaCl, 2.5 KCl, 0.8 $MgSO_4$, 0.9 NaH_2PO_4, 1.8 $CaCl_2$, 5.5 dextrose, and 10 HEPES (pH 7.4). They were fixed in 1.0% glutaraldehyde in BSS, stained in 1% osmium tetroxide, dehydrated from ethanol to freon-113® by the exchange method, and critical-point dried. This treatment produced a shrinkage of about 35%. After a 5-nm layer of gold palladium was deposited, the cells were photographed in an ISI Model DS-130 scanning electron microscope fitted with an LAB-6 lanthanum hexaboride electron emitter (courtesy of R. Apkarian, SEM Laboratory, Yerkes Regional Primate Research Center, Emory University.)

Solutions

The trypsin dissociation solution contained crystalline trypsin, 50 μg/ml, deoxyribonuclease, 5.5 μg/ml (both from Cooper Biomedical), and bovine serum albumin (Miles Lab, Fraction V, fatty acid poor, 1 mg/ml) dissolved in PBSS. Collagenase solution was the same as above except that trypsin was replaced by collagenase 4177 CLS II (Cooper Biomedical, 2 μg/ml). The low-Ca solution for dissociation of 2d hearts without enzymes contained (in mM): NaCl 120, KCl 5, NaH_2PO_4 0.4, Na_2HOP_4 1, dextrose 5.5, $CaCl_2$ 18 μM, pH 7.4. The culture medium (M21212) consisted of 25% M199, 2% heat-inactivated selected horse serum, 4% fetal calf serum, 68.5% K-free Ham's F12 (all from Grand Island Biological), penicillin-G (5 units/ml) and KCl (final concentration, 4.3 mM).

In early experiments the buffer solution used to bathe the cells for electrical measurements contained (in mM): NaCl 116,

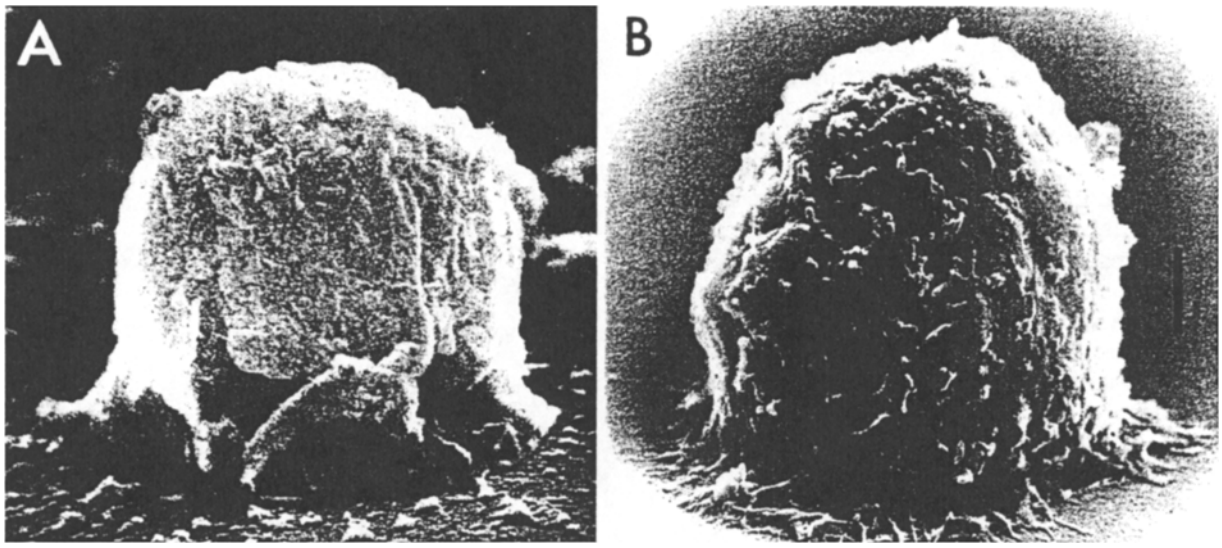

Fig. 1. Scanning electron micrographs of chick ventricle cells. (*A*) 2d + 1 and (*B*) 7d + 1 cells typical of those used in the present study, viewed tilted 70° from vertical. Total shrinkage during preparation was about 35% (*see* Materials and Methods). Scale = 1.6 μm in (*A*) and 2 μm in (*B*)

KCl 4.3, $MgSO_4$ 0.8, $CaCl_2$ 1.8, NaH_2PO_4 0.9, $NaHCO_3$ 26.3, dextrose 5.5. In these cases experiments were performed in an atmosphere of 5% CO_2, 10% O_2, 85% N_2. However, most of the data were obtained from cells in an ungassed solution in which NaCl was increased to 142 mM and bicarbonate was replaced by 10 mM HEPES buffer, pH 7.4.

Three intracellular perfusion solutions were used in the electrodes. These contained (in mM): NaCl 10, 20, 15; K-glutamate 95, 125, 120; NaH_2PO_4 0.9, 0.9, 0; $NaHCO_3$ 26, 0, 0; $MgCl_2$ 1, 4, 4.6; EGTA 5, 11, 5; $CaCl_2$ 0, 1, 0.068; HEPES 10, 10, 10; ATP 3, 3, 3; creatine phosphate 3, 3, 3; pH 7.4, 7.4, 7.1. Sodium equilibrium potential (E_{Na}) for these solutions, with 142.9 mM Na^+ in the bath was, respectively, 22, 37, and 42 mV.

Recording Procedures

Cells were washed extensively with balanced salt solution and maintained on a temperature-controlled microscope stage at 22 ± 1°C for experiments. Patch electrodes were drawn from glass capillaries (Drummond Microcaps, 100 μl) to resistances of 2 to 6 MΩ according to well-described methods (Sakmann & Neher, 1984), coated with Sylgard® (Corey & Stevens, 1983), and filled with internal perfusion solution. Gigaohm seals were achieved on isolated 13 to 18 μm diameter cells. After the membrane patch was disrupted, satisfactory access to the cell interior and adequate voltage control through the Dagan model 8900 patch-clamp amplifier, were judged by obtaining a capacitive charging current with a single-exponential decay having a time constant of less than 60 μsec, and a peak current indicating a series resistance (R_{ser}) of 5 to 10 MΩ. Capacitive charging currents were recorded directly on diskette using a Nicolet 4094 digital oscilloscope with wide band pass filtering at >10 kHz. Current responses to voltage-clamp steps were recorded with an analog FM magnetic tape recorder (HP-3968A) with lowpass filtering at 5 kHz or were digitized and recorded on VCR tape (Neurocorder model DR-484) at 22 kHz sampling rate. Sequences of 400 msec voltage-command steps were provided by a programmable digital signal generator designed and built in this laboratory.

Net I_{Na} was obtained by subtracting either the leak current measured 80 msec after the voltage step, or in some cases, the residual current in 150 or 300 nM TTX. Subtraction of the TTX-resistant components from the total fast inward current usually made little difference in the current shape or kinetics (*see below*). *I/V* curves were determined by measuring net I_{Na} activated from a 3.6-sec holding potential (V_{Hold}) of −80 mV by command potentials (0.4-sec duration) in the activation range from −60 to +80 mV. Net sodium conductance (G_{Na}) was calculated as $I_{Na}(V)/(V - E_{Na})$ and, when normalized to peak conductance (G_{Na} max), was considered to equal steady-state activation (m_∞). The steady-state inactivation of I_{Na} (h_∞) was measured with 0.4-sec voltage-clamp command steps (V_{com}) to −20 mV from 3.6-sec conditioning prepulses in the range from −130 to −50 mV. Plots of normalized peak current against V_{Hold} were made to illustrate the steady-state voltage dependence of h_∞. Both steady-state activation and inactivation data were fit to a logistic function, with a nonlinear least-squares fitting program using the Marquardt algorithm, implemented on the IBM PC-AT computer. A convenient parameter for comparing inactivation curves from different cells was V_h, the holding potential from which 50% of the sodium current could be activated ($h_\infty = 0.5$).

Results

Cell Structure and Passive Properties

Rounded cells (Fig. 1) with diameters of 13 to 18 μm were selected for application of patch electrodes at all stages. Virtually all of these cells at all stages beat spontaneously in M21212. For voltage-clamp analysis, cells were washed in BSS, a patch-elec-

trode gigaseal was established, and the capacitive charging current (I_{cap}) of the electrode and unbroken patch was compensated. After disrupting the patch, I_{cap} increased in amplitude, and typically decayed monoexponentially in less than 250 μsec with a time constant (τ_{cap}) < 60 μsec for both 7d (Fig. 2*A*) and earlier (Fig. 2*B*) cells. Selection by the criteria of sphericity and size yielded populations of cells that were comparable in passive properties at all stages. Mean cell input resistance, determined from the slope of the steady-state *I/V* at −60 mV, was 5.2 ± 1.1 GΩ (mean ± SE, N = 9 2d, 4 3d, 1 4d, and 9 7d) consistent with specific membrane resistance of 20 to 40 kΩcm² (Clay, DeFelice & DeHaan, 1979). From a total of 221 cells of the four ages, whose surface area was estimated both visually (with an optical reticle), and by G_{in}, we calculated a mean value (±SD) of 7.46 ± 3.50 pF/cell, and 0.90 ± 0.32 μF/cm² for specific membrane capacitance. There were no significant differences among the age groups in these parameters (Fig. 3*A–D*).

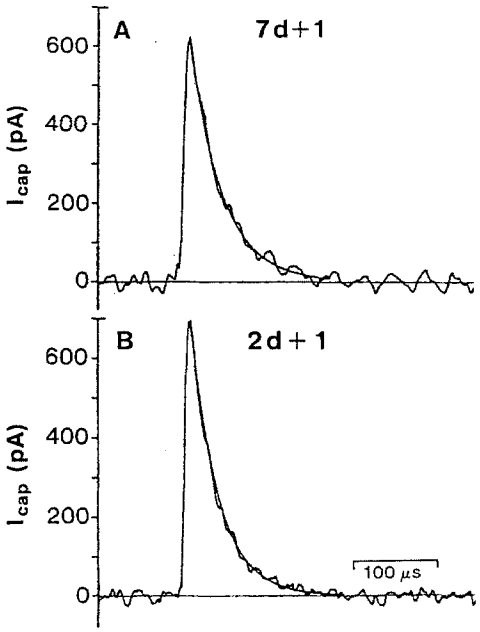

Fig. 2. Measurement of cell capacitance (C_{in}). (*A*) Capacitive charging current (I_{cap}) in response to a 10-mV V_{com} step from a 15-μm diameter 7d + 1 cell after the membrane patch was disrupted. Fitting the current decay to a monoexponential curve gave: C_{in}, 6.3 pF; R_{ser}, 6.1 MΩ; visual surface area, 707 μm²; C_m, 0.92 μF/cm². The decay phase of the current is superimposed on the exponential curve with τ = 38.7 μsec. (*B*) I_{cap} from a 16-μm 2d + 1 cell after system compensation and patch disruption as above: C_{in}, 6.5 pF; R_{ser}, 5.1 MΩ; visual surface area, 804 μm²; C_m, 0.81 μF/cm². The decay phase of the current is superimposed on the exponential curve with τ = 32.7 μsec

Voltage-Clamp Analysis of I_{Na}

From V_{Hold} = −80 mV, depolarizing command potentials elicited fast inward currents in 7d + 1 cells (Fig. 4*A*) that reached a peak in less than 1 msec over the voltage range from −20 to +40 mV. Maximal current in the example shown is 1370 pA at −20 mV. The same command potentials (Fig. 4*C*) activated similar current of smaller magnitudes in 4d + 1, 3d + 1, and most 2d cells including 2d + 1, 2d + 14–16h and 2d + 6–8h cells (isolated by maceration in low-Ca buffer without enzymes). A family of currents from a 2d + 1 cells is shown in Fig. 4(*B*). I_{Na} was present in all 3d + 1, 4d + 1 and 7d + 1 cells tried, but in only 55% of the 2d + 1 cells. In a few cells at all ages, a calcium current could be observed immediately after disruption of the membrane patch, but this quickly disappeared, presumably because our electrode-filling solutions lacked cAMP.

The peak current-voltage (*I-V*) relations of the cells depicted in Figs. 4(*A*) and 4(*B*) are represented in Fig. 4(*D*). From the families of current responses and the *I-V* curves, it is apparent that the currents are qualitatively similar in 2d and 7d cells. However, quantitative differences in amplitude, voltage dependence and in kinetics of the currents were observed with development.

(*a*) *Increase of Current Density with Development*

The most dramatic systematic change of I_{Na} with development age was in its magnitude. Representative currents elicited by a step from −120 to −20 mV increased progressively with developmental age (Fig. 5*A*). The voltage dependence of I_{Na} in representative cells is seen by scaling the currents to C_{in}, and plotting the *I/V* curves in terms of specific membrane current density (Fig. 5*B*). The mean magnitude of the fully saturated current, plotted as a function of developmental age (Fig. 5*C*) shows that current density grew about eightfold between 2d + 6h and 7d + 1 cells (Table 1, columns 1, 5, 6).

(*b*) *Time-Dependence of Sodium Current Activation and Inactivation*

At all stages tested, the time for sodium current activation depended on V_{com}. At potentials positive to about −30 mV, activation was rapid; time to peak (T_P) was less than 1 msec in all cells older than 2d + 8h. T_P showed a decreasing trend with developmental age but the differences were not statistically significant (Table 1, column 7). Because the activation process overlapped the decay of the capacitive charging current, an accurate measure of

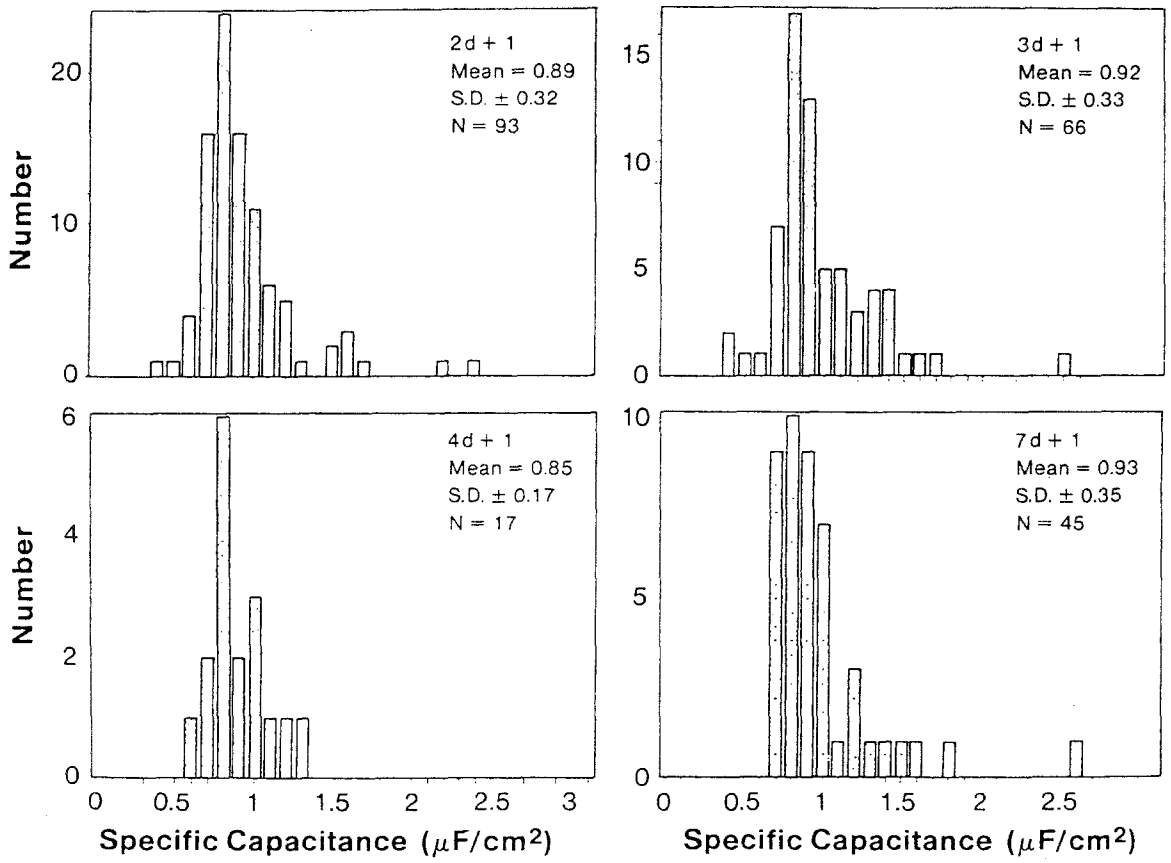

Fig. 3. Frequency histograms of specific capacitance. Mean specific capacitance (μF/cm^2) of all cells in which a successful gigaseal and patch disruption were achieved, with standard deviation and number of cells (N) given for each group. Further analysis of current properties was performed on only a fraction of these cells

Table 1. Developmental changes in sodium current parameters (mean ± SD)

1 Age	2 N	3 Diameter (μm)	4 C_{in} (pF)	5 $I_{Na(sat)}$[a] (pA)	6 $I_{Na(sp)}$[a] (μA/μF)	7 T_P[a] (msec)	8 τ_h[a] (msec)	9 V_h (mV)	10 K_h (mV)
2d ± 8h[b]	2	14.8	6.8	199	28	1.09	1.95	—	—
2d ± 16h[c]	4	16.8 ± 1.1	8.8 ± 1.2	352 ± 183	39 ± 17	0.91 ± 0.16	1.29 ± 0.2	—	—
2d ± 1[d]	41	15.8 ± 1.6	8.0 ± 1.7	312 ± 247	40 ± 34	0.84 ± 0.19	1.47 ± 0.5	−78.8 ± 9.5[e](29)	7.7 ± 3.4[e](29)
3d ± 1[d]	27	16.5 ± 1.0	8.6 ± 1.1	971 ± 762	114 ± 96	0.79 ± 0.20	1.80 ± 0.6	−79.1 ± 6.3[e](15)	7.2 ± 0.8[e](15)
4d ± 1[d]	12	15.8 ± 1.6	7.9 ± 1.8	1237 ± 586	161 ± 84	0.64 ± 0.18	1.15 ± 0.4	—	—
7d ± 1[d]	25	15.2 ± 1.0	7.3 ± 1.1	1550 ± 595	219 ± 87	0.69 ± 0.09	0.99 ± 0.2	−86.4 ± 9.7[e](46)	8.5 ± 6.1[e](46)

[a] Step from $V_{Hold} = -120$ mV to $V_{com} = -20$ mV.
[b] Cells were dissociated by mechanical maceration in low-Ca phosphate buffer without exposure to enzymes. Recordings were made after 6 to 8 hr of incubation at 37°C in M21212.
[c] Measurements were made 14 to 16 hr after dissociation in trypsin or collagenase.
[d] Measurements were made 23 to 28 hr after dissociation in trypsin or collagenase.
[e] SEM.

the activation time constant (τ_m) could not be made. Based on T_P, however, τ_m was probably less than 0.3 msec at V_m positive to −30 mV even in the slowest cells.

The kinetics of I_{Na} decay were also voltage-dependent, according to the familiar Hodgkin-Huxley pattern. In most cells, at all ages, inactivation followed a monoexponential time course (Fig. 6*A*,*B*), and was accelerated by depolarization of the membrane. Although there was great variation from cell

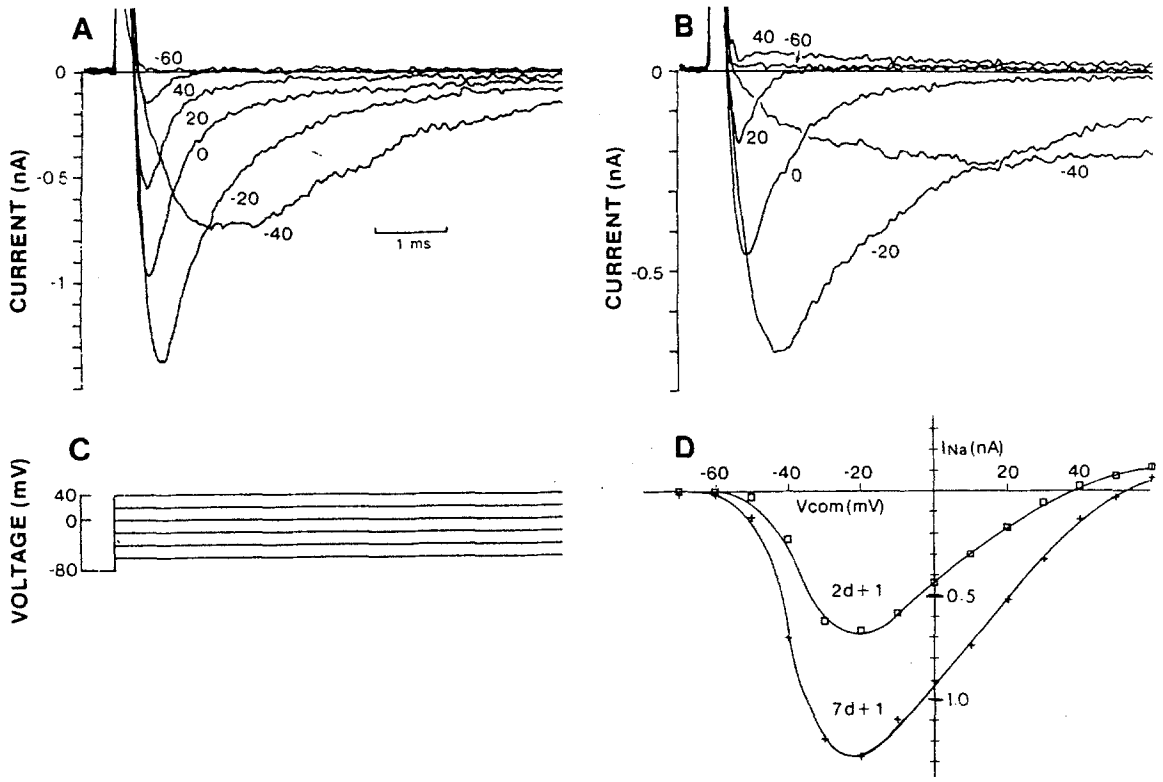

Fig. 4. Voltage dependence of I_{Na}. Superimposed fast current responses of (*A*) 7d + 1, and (*B*) 2d + 1 cells to (*C*) voltage-command steps from $V_{Hold} = -80$ mV to sequential levels from −60 to +40 mV; only the 20-mV increment steps are shown. Duration of V_{com} and V_{Hold} were 0.4 and 3.6 sec. The 1-msec scale in (*A*) applies to both (*A*) and (*B*). Currents have been corrected digitally to remove linear leak. (*D*) *I/V* curves constructed from the peak currents obtained from the cells in (*A*) and (*B*). The pipettes on the cells shown in (*A*) and (*B*) contained solutions with $E_{Na} = 37$ and 42 mV, respectively. C_{in} was 6.79 and 7.94 pF

to cell, the time constant for inactivation (τ_h) was longest in 2d cells, and decreased with developmental age (Fig. 6*C*). For example, mean τ_h for the step from −120 to −20 mV in 7d + 1 cells (0.99 msec) was only about half that of two 2d cells measured 6 to 8 hr after dissociation (1.95 msec; Table 1, column 8).

(*c*) *Steady-State Inactivation of* I_{Na}

When V_{Hold} was positive to about −60 mV, the fast inward current was blocked. As V_{Hold} was made more negative, more current could be activated. This voltage dependence of steady-state sodium current inactivation (h_∞) was measured by applying conditioning prepulses in the range −120 to −50 mV to the cell before stepping to a command potential at −20 mV. The responses of cells at different ages were similar but not quantitatively identical. The currents from a 7d + 1 and a 2d + 1 cell are shown as examples (Fig. 7). The peak currents from similar cells are plotted as a function of prepulse potential (Fig. 8, left-hand curve) after normalization to the saturating current elicited by maximal hyperpolarization (from −120 or −130 mV) in each cell. V_h for 7d + 1 preparations averaged about 7 mV more negative than for 2d + 1 or 3d + 1 cells, but this apparent difference was not significant because of the large cell-to-cell variation (Table 1, column 9). Therefore, only a single sigmoidal curve is fit to all the points in Fig. 8.

(*d*) *Steady-State Activation of* I_{Na} *and Calculation of* $\bar{G}_{Na}$

To compare I_{Na} activation in cells at different ages, G_{Na} was determined by dividing values of peak I_{Na} elicited by steps to various command potentials, as described above, by the driving force on sodium ($V_m - E_{Na}$). G_{Na}, normalized with respect to the maximum value for each cell, was taken as equivalent to steady-state activation (m_∞). In Fig. 8 (right-hand curve), G_{Na}/G_{Na}max is plotted as a function of V_m (command potential) for the same cells represented in the inactivation curves. The activation curves clustered around $V_{mid} = -30$ mV.

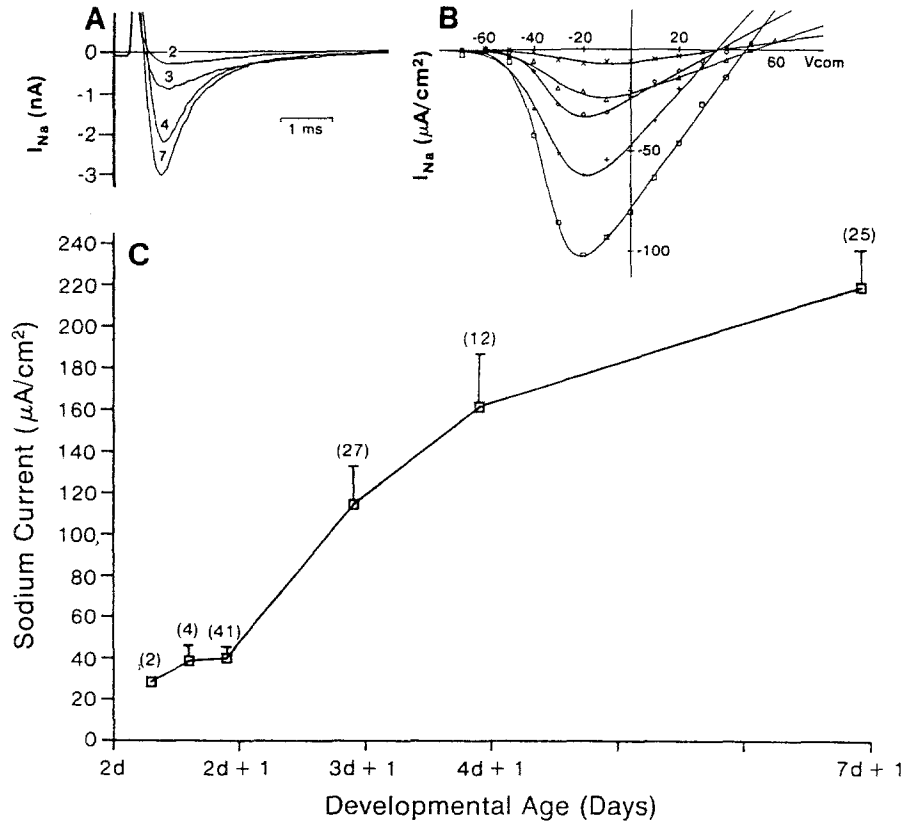

Fig. 5. Increase in I_{Na} in cells of different ages. (*A*) Superimposed net currents from a 2d + 1, 3d + 1, 4d + 1 and 7d + 1 cell (top to bottom traces) in response to a voltage pulse from −120 to −20 mV. In each case, the current has been corrected digitally for leak current. (*B*) *I/V* curves of net I_{Na} obtained from typical 2d + 8h, 2d + 1, 3d + 1, 4d + 1 and 7d + 1 ventricle cells, from V_{Hold} = −80 mV to the command potentials indicated on the voltage axis. For the 2d + 1 and 7d + 1 cells, the electrode filling solution contained 27 mM Na^+ (E_{Na} = 42 mV); for the other three ages shown, it contained 33 mM Na^+ (E_{Na} = 37 mV). This accounts for the difference in current reversal potentials. The currents were normalized to C_{in} and are plotted as specific membrane current density. The continuous curves were calculated from the fit of the m_x data. (*C*) Maximal sodium current evoked by steps from V_{hold} = −120 mV to V_{com} = −20 mV, from cells of different developmental ages. Mean and standard error bars are shown, with the number of cells (*N*) in parentheses near each error bar

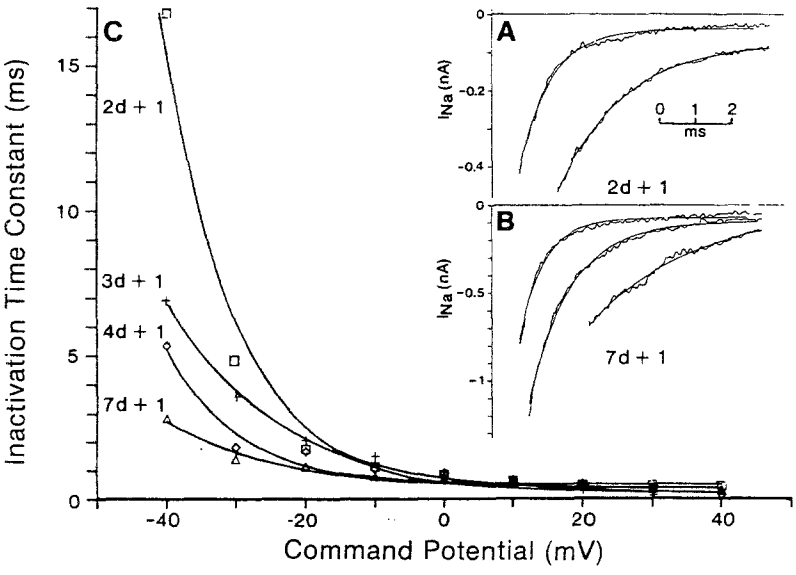

Fig. 6. Time dependence of I_{Na} inactivation (τ_h). Decay of I_{Na} activated from V_{hold} (−80 mV) to (*A*) −20 and 0 mV, in a 2d + 1 cell, and (*B*) to −40, −20 and 0 mV, in a 7d + 1 cell. Each current is fit to a monoexponential function; the inactivation time constants are, respectively, (*A*) 1.7 and 0.8 msec; and (*B*) 2.8, 1.1 and 0.7 msec. (*C*) τ_h of a representative 2d + 1, 3d + 1, 4d + 1 and 7d + 1 cell, as a function of V_{com}. The smooth curves connecting the experimental values are monoexponential functions

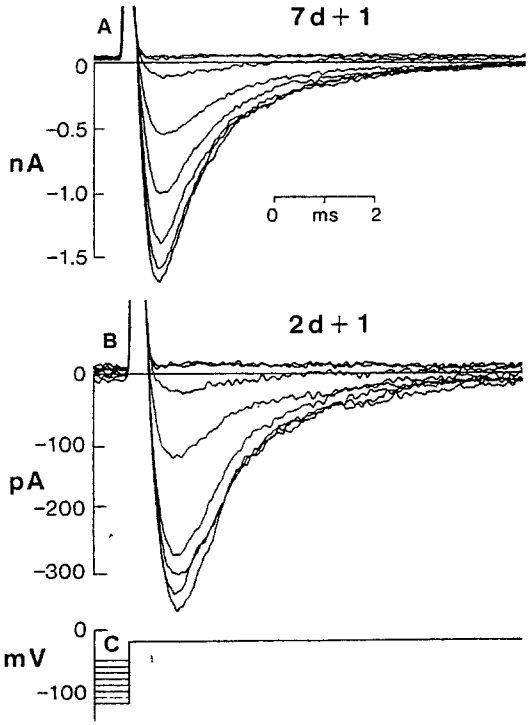

Fig. 7. Steady-state voltage-dependent inactivation of I_{Na}. Superimposed fast current responses of (*A*) 7d + 1 and (*B*) 2d + 1 cells to (*C*) a 400-msec voltage command potential of −20 mV, from 3.6-msec sequential steps at V_{Hold} = −120 to −50 mV. The saturating current (h_∞ = 1.0) was 1710 pA for the 7d + 1 cell and 373 pA for the 2d + 1 cell. These records have not been corrected for leak or other contaminating currents. C_{in} of these cells was 6.34 and 6.20 pF, respectively

The value for sodium conductance in the absence of inactivation, $\bar{G}_{Na}$, was estimated from an extrapolation of I_{Na} (I_{Nao}) back to the beginning of the command step at voltages in the range where m_∞ was at or near unity, and τ_h was much longer than τ_m (V_{com} = −20 to 20 mV). This extrapolation of the exponential decay of the current (Fig. 6*A*,*B*) gave $I_{Nao}h_o m_\infty$, where h_o is the initial value of h at the beginning of the pulse (i.e., h_∞ at V_{Hold}). The values for h_o were computed from the h_∞ equation (legend to Fig. 8) for each cell. The maximal available current is then:

$$\bar{G}_{Na} = I_{Nao}h_o m_\infty/[h_o m_\infty(V_m - E_{Na})].$$

The values of $\bar{G}_{Na}$ for the 2d + 1 to 7d + 1 cells chosen for analysis in Fig. 6 are (in order of increasing age): 64.2, 71.9, 58.5, and 148.8 nS. Scaling these values at each age by the fraction: mean $I_{Na(sp)}/I_{Na(sp)}$ (where mean $I_{Na(sp)}$ was taken from Table 1, col. 6), gave the averages listed in Table 2.

Table 2. Calculated average $\bar{G}_{Na}$ and sodium channel density

Age	$\bar{G}_{Na}$ (nS)	$\bar{G}_{Na(sp)}$ (mS/cm²)	*N*/cell	*N*/μm²	$G_{Na(sat)}$[a] (nS)
2d + 1	18.6	2.3	1240	1.6	5.5
3d + 1	32.4	3.8	2160	2.5	14.7
4d + 1	36.9	4.7	2460	3.1	18.7
7d + 1	140.0	19.3	9330	12.9	25.0

[a] Average peak conductance during a step from V_{Hold} = −120 mV to V_{com} = −20 mV.

Tetrodotoxin Sensitivity of I_{Na}

The fast inward current was blocked by TTX at all stages tested. Subtracting the residual current evoked in 150 nM TTX (Fig. 9*A*,*B*, trace 2) from the total membrane current (trace 1), to leave net I_{Na} (trace 3) afforded only a small, or no correction, in most cases. Moreover, cells of different ages demonstrated no substantial differences in sensitivity to the toxin, nor did those dissociated with trypsin versus collagenase. In these experiments, complete TTX dose-response curves were not obtained on any given cell. With most cells, after recording current parameters in control buffer and in two or three different concentrations of toxin, the seal was lost or the preparation died. However, by pooling data from several cells of each age, it was possible to obtain a relation between TTX concentration and percent inhibition of sodium current for 2d + 10h, 2d + 1, 3d + 1 and 7d + 1 cells. The two sigmoid curves through the points in Fig. 10 are based on pooled data from 12 cells from 2 to 3d hearts, and from two 7d + 1 cells. The concentration required for half-maximal suppression of the current ($K_{0.5}$) for the four age groups was: 0.46, 0.56, 0.63, 0.85 nM. The data for the younger stages were therefore averaged. The difference in $K_{0.5}$ between the pooled 2 to 3d cells (0.58 nM) and the 7d + 1 cells (0.85 nM) was also not significant.

Discussion

Properties of the Developing Sodium Current

Since the classic description by Hodgkin and Huxley (1952), I_{Na} has been recognized in a variety of adult excitable cells. Identifying characteristics of the current include its rapid kinetics, the dependence of its peak magnitude and reversal potential on $[Na^+]_o$, its sensitivity to block by an inactivating

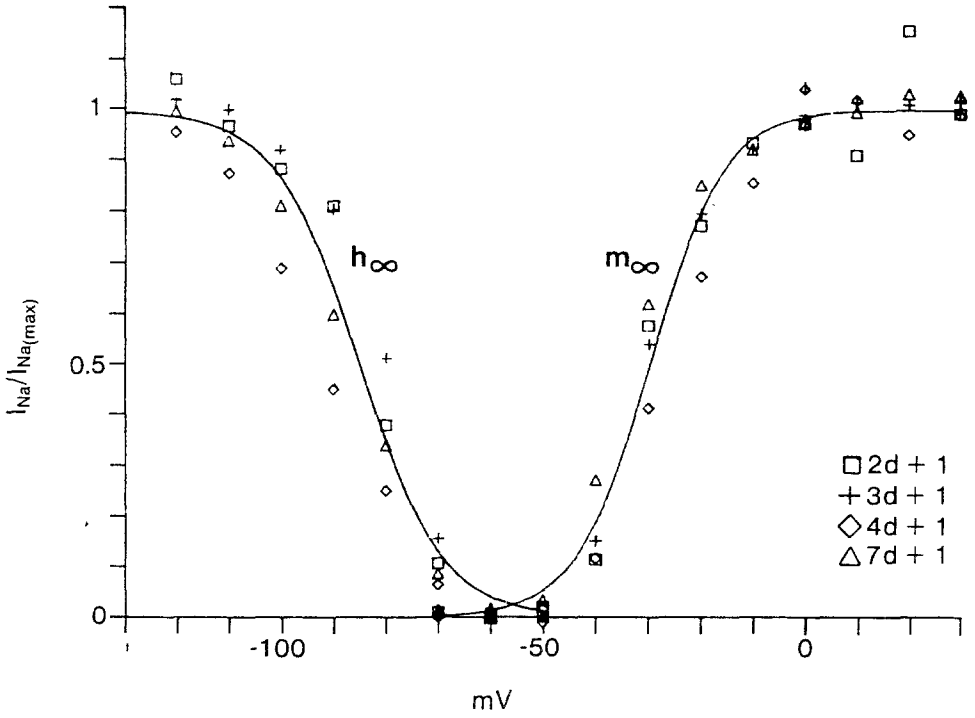

Fig. 8. Voltage-dependence of sodium current inactivation and activation. Normalized steady-state sodium inactivation (left-hand) and activation (right-hand) curve. Data points for a 2d + 1, 3d + 1, 4d + 1, and 7d + 1 cell are shown. The sigmoidal dependence of I_{Na} inactivation on prepulse potential, and of activation on V_{com} have been fit by the sigmoidal logistic functions (Hodgkin & Huxley, 1952): $h_\infty = 1/[1 + \exp((V - V_h)/k_h)]$ (inactivation); $m_\infty = 1/[1 + \exp((V_{mid} - V_{com})/k_m)]$ (activation), where V_h and V_{mid} are the potentials at which h_∞ and $m_\infty = 0.5$, and k_h and k_m are defined as the number of millivolts for an e-fold change along the curves. The calculated values defining the inactivation and activation curve for the 2d + 1, 3d + 1, 4d + 1, and 7d + 1 cells, respectively, are: $V_h = -82.7$, -80.4, -92.0, -86.8 mV; $k_h = 5.9$, 6.5, 9.4, 8.3 mV; $V_{mid} = -30.0$, -30.0, -28.0, -32.8 mV; $k_m = -6.4$, -6.5, -7.6, -6.9 mV

prepulse or by TTX, and the shape and voltage range of its *I/V* relation. The whole-cell voltage-clamp results reported here indicate that a voltage-activatable current with characteristics that identify it as I_{Na} is present in cells of the embryonic chick ventricle from at least two days of development. This early current is qualitatively similar to that in the 7d + 1 cell, and resembles closely the I_{Na} identified in other cardiac preparations (Colatsky, 1980; Ebihara et al., 1980; Brown et al., 1981). Nonetheless, our results provide evidence for systematic changes with development in current density and in inactivation kinetics.

Developmental Increase in Current Density and Number of Sodium Channels

The maximal sodium current ($I_{Na(sat)}$) that could be activated in two early 2d cells (2d + 6h, 2d + 8h) averaged 28 μA/μF (Fig. 5; Table 1, column 6). During the next two days of development (to 4d + 1), a sixfold increase occurred, to 160 μA/cm^2. By seven days, maximal I_{Na} had increased eightfold over the 2d + 6–8h value, to 219 μA/cm^2. The latter value is in fair agreement with results from 7d ventricle cell aggregates (Nathan & DeHaan, 1979), and from neonatal rat heart cells (Cachelin et al., 1983; Kunze et al., 1985).

Hodgkin and Huxley (1952) defined $\bar{G}_{Na}$ as the maximal sodium conductance available in the absence of inactivation. We estimated $\bar{G}_{Na}$, at each age, from currents activated at potentials where m_∞ was at or near unity, and where τ_h was large relative to τ_m. τ_m was approximated as 0.3 T_P, consistent with records published by Ebihara and Johnson (1980). Extrapolating the exponential decay of the current at these potentials back to zero time, gave $I_{Na_o} h_o m_\infty$ (I_{Na} at $m = m_\beta$, and $h_o = h_\infty$ at V_{Hold}). As shown in Table 2, $\bar{G}_{Na(sp)}$ increased eightfold during the first week of development, from 2.3 mS/cm^2 in 2d cells to 19.3 mS/cm^2 in 7d cells. The latter value agrees well with the results of Ebihara and Johnson (1980), who measured 21.8 mS/cm^2 for the average maximal sodium conductance in three 11d chick heart cell clusters.

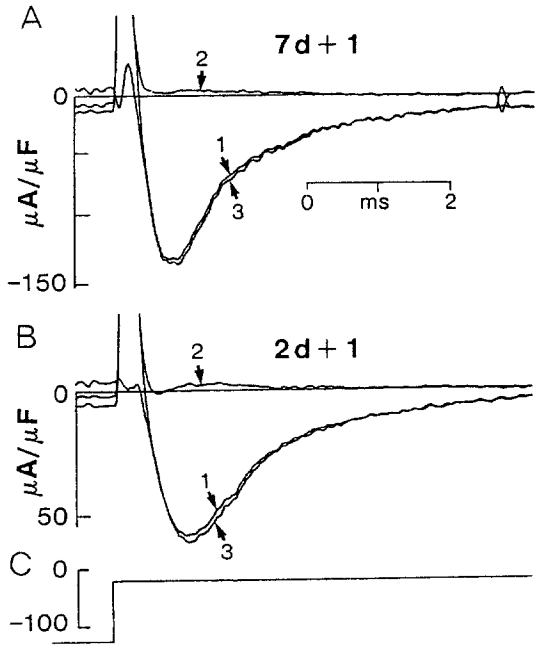

Fig. 9. TTX block of the fast inward current. Current responses in (*A*) a 7d + 1 and (*B*) a 2d + 1 cell to (*C*) a voltage step from $V_{Hold} = -120$ mV to $V_{command} = -20$ mV, before (trace 1) and in the presence of 150 nM TTX (trace 2). The difference current (trace 3) represents net I_{Na} uncontaminated by leak or by other TTX-resistant currents. Similar responses were seen in cells from all stages tested, though in some early cells the decay time for I_{Na} was appreciably reduced after correction

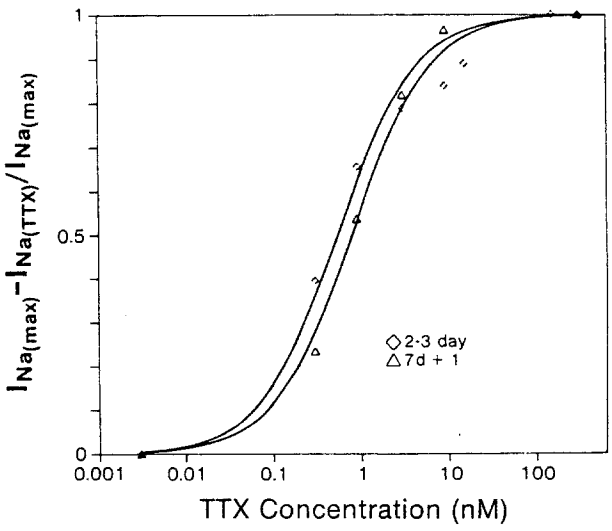

Fig. 10. Dose response to TTX. The inhibition of I_{Na} is plotted as a function of TTX concentration for 12 2 to 3d cells (two 2d + 10h, four 2d + 1, and six 3d + 1), and two 7d + 1 cells. Fractional inhibition is measured as (I_{Na}max − I_{Na}TTX)/I_{Na}max. The data points are pooled and fit to the equation: Relative Inhibition = [TTX]/($K_{0.5}$ + [TTX]), where $K_{0.5}$ is the concentration of TTX that produced half-maximal inhibition

Sodium conductance may be defined as $\gamma_{Na}NP_o$, where N is the number of sodium channels per cell, γ_{Na} is single-channel conductance, and P_o is the open-state probability of the channels. Values for γ_{Na}, measured in cell-attached or excised patches of a variety of cardiac cell membranes have been to 10 to 20 pS (Cachelin et al., 1983; Ten Eick, Yeh & Matsuki, 1984; Kunze et al., 1985; Makielski et al., 1987), not appreciably different from those reported from noncardiac cells (Fenwick, Marty & Neher, 1982). In single-channel terminology, $\bar{G}_{Na}$ is the sodium conductance under the condition that $P_o = 1$. Therefore, $N = \bar{G}_{Na}/\gamma_{Na}$. Taking $\gamma_{Na} = 15$ pS, we calculated (Table 2) that there are about 1200 channels in 2d + 1 cells ($N/\mu m^2 = 1.6$). That number increases to over 9000 ($13/\mu m^2$) in an average 7d + 1 cell, with a variation from cell to cell of about 40%. Applying a modified Hodgkin-Huxley model to action currents from 7d + 1 cells identical in preparation to those used in the present study, Mazzanti and DeFelice (1987) recently calculated that total sodium channel density was about $20/\mu m^2$ (15,000/cell) while Ebihara and Johnson (1980) estimated 11 to 20 channels/μm^2 in small cell aggregates of 11d chick heart. A similar increase in channel density apparently occurs during postnatal development in the rat heart. There are 1 to 2 channels/μm^2 in cultured neonatal rat cardiac myocytes (Cachelin et al., 1983; Kunze et al., 1985), while isolated cells from adult rat heart contain $16/\mu m^2$ (Brown et al., 1981 calculated by Cachelin et al., 1983). Using STX binding as a means of counting channels, Doyle et al. (1985) found 4 to 8 binding sites per μm^2 of sheep heart plasma membrane. These values are to be compared with 5 to $15/\mu m^2$ in different noncardiac cell types in culture (Fenwick et al., 1982), and 200 to $300/\mu m^2$ in canine cardiac Purkinje fibers (Makielski et al., 1987) and in squid axon (Bekkers, Greeff & Keynes, 1986).

Up to about 30h of development, the heart is represented in the chick embryo only by undifferentiated precardiac mesoderm. No information exists on when transcription of cardiac sodium channel mRNA begins as these cells differentiate during the second day of incubation. However, by the end of that day, our results show that sodium channel density is already 1200/cell, and it increases to 9300/cell over the next five days of development. In fetal mouse brain, neurotoxin-sensitive sodium channels increase about sixfold from 11 days to 19 days of gestation (Courad et al., 1986) and about eightfold in the first three weeks after birth in rat brain (Lombet et al., 1983). These results suggest that channel protein may be synthesized and inserted into the cell membrane at rates of 50 to 100 molecules/hr during certain periods. Using specific polyclonal antibodies against the rat brain channel, Schmidt and

Catterall (1986) have shown that it takes about 2 hr for newly synthesized α-subunits, disulfide-linked to β-2 subunits, to begin to appear as functional sodium channels in the membrane of cultured rat brain neurons. The α-subunit DNA contains about 2000 codons (Noda et al., 1986). Translation rates per ribosome of 1.5 codons/sec (5000/hr) are not unusual in embryonic cells. With 5 ribosomes/mRNA, it would require only 20 mRNA's to produce 100 channel proteins/hr. With a large amount of injected chick muscle mRNA, Sigel (1987) has achieved synthesis of functional sodium channels in *Xenopus* oocytes at the rate of 20/sec/oocyte.

Kinetics and Voltage Dependence of the Sodium Current

Voltage-clamp steps from V_{Hold} into the range positive to about −60 mV caused the activation of families of currents whose magnitudes, and rate of onset and decay were strongly dependent on V_{com}. The examples from a 2d + 1 and a 7d + 1 cell in Fig. 4 suggest that the activation phases of the currents were similar in cells from all ages analyzed. We found that T_P and the activation voltage ranges were similar at all ages (Figs. 4, 5*B*; Table 1, column 7), and that the midpoint of the m_∞ curves clustered around −30 mV (Fig. 8). This is near the values found with two-electrode voltage clamps in rabbit Purkinje fiber (Colatsky, 1980) and in 11d chick embryo heart cell aggregates (Ebihara & Johnson, 1980).

Inactivation kinetics were more variable from cell to cell, but showed significant changes with development. At potentials negative to zero, τ_h in 7d + 1 cells was on average 1.5 times faster than in 2d + 1 cells, and twice as fast as in 2d + 6–8h cells (Table 1, column 8). In most cells, inactivation could be fit by a monoexponential function, and was not appreciably altered by subtracting the TTX-resistant component. These results suggest that up to seven days embryonic ventricle cells have only a single class of functional sodium channels, with a single inactivation state. In contrast, the 11-day chick heart is reported to have an additional class of slowly inactivating sodium channels (Ebihara & Johnson, 1980; Ten Eick et al., 1984), as do adult mammalian cardiac cells (Brown et al., 1981; Kunze et al., 1985; Patlak & Ortiz, 1985; Follmer, Ten Eick & Zeh, 1987).

With patch electrodes that allow free diffusional access between the electrode-filling solution and the cytosol, V_h has been found to shift to a more negative voltage range than it has when the analysis is done with traditional high-resistance electrodes (Fernandez, Fox & Krasne, 1984; Kunze et al., 1985; Follmer et al., 1987). This shift has been attributed to diffusion of charged macromolecules from the cytoplasm into the pipette. In 11-day chick heart cell clusters impaled with high-resistance intracellular electrodes, Ebihara and Johnson (1980) measured V_h at −69 mV. In patch-clamped single chick ventricle cells, we found V_h shifted to −79 mV at 2d and −86 mV in 7d cells (Table 1, column 9). Similar variability in V_h has been seen in other preparations as well. Using intracellular electrodes in mammalian cardiac tissue, Beeler and Reuter (1970) reported V_h at −56 mV, while more recent measurement have given substantially more negative values, from −75 to −90 mV (Colatsky, 1980; Cohen, Bean & Tsien, 1984; Kunze et al., 1985). The position of the inactivation curve along the voltage axis depends on experimental conditions. Cooling shifts V_h in a negative direction (Colatsky, 1980). Increasing external Ca or acidifying the bath solution have an opposite effect (Hahin & Campbell, 1983; Campbell & Hahin, 1984). V_h is also under the influence of external cell surface components, since initiating flow in the external bath can cause a negative shift in the h_∞ curve (Ayer, Fujii & DeHaan, 1985). Such shifts can even occur in cell-attached patches (Kunze et al., 1985). Thus, it is not clear whether differences in V_h between 7d + 1 and 2d + 1 cells result from a developmental change in the inactivation mechanism, or from a greater susceptibility of the 7d cells to those experimental conditions that produce a negative shift. The mean difference of 7 mV in V_h between 2d and 7d cells is not large enough to account for more than a small part of the twofold difference in inactivation kinetics. A shift of more than 20 mV would be required to produce the change seen in Fig. 6(*C*), but such large differences in V_h between the two ages were rarely seen.

Adequacy of Voltage Control

In any discussion of the properties of I_{Na}, the series resistance (R_{ser}) artifact and adequacy of voltage control must be considered. If R_{ser} is large, the negative slope branch of the *I/V* curve and the voltage-dependent rate constants of the Na system are distorted and shifted to the left along the voltage axis. Several methods for assessing adequacy of voltage control are available (Fozzard et al., 1985).

The time constant of the decay of the capacitive charging current in response to a small voltage step is determined primarily by the product of R_{ser} and the cell input capacitance. The fastest published decay times for voltage clamp of single cardiac cells are in the range of 15 to 80 μsec (Brown et al., 1981; Bustamente & McDonald, 1983; Makielski et al., 1987). As shown in Fig. 2, we have used a monoexponential decay time constant <60 μsec in response

to a 10-mV pulse as a worst-case criterion for acceptance in the present study. In most cases, τ_{cap} was about half that. The access resistance giving a 30-μsec capacitive time constant for a 7.5-pF cell is 4 MΩ. Compared with a resting cell input resistance of 5 GΩ, this much series resistance was tolerable. Moreover, other criteria indicated that voltage-clamp control of the cells was adequately fast. These included the speed of onset of current activation (<1 msec), and its striking voltage dependence (Fig. 4), the gradualness of the increase of the current with depolarization in the negative slope limb of the *I/V* curves, and the constancy of shape of these curves over a wide range of current densities (Fig. 5*B*).

An additional severe test for R_{ser} was performed on each cell by varying the current magnitude with inactivating prepulse potentials. Over a 10-fold range in I_{Na}, no appreciable change in current kinetics could be observed, as manifested in time to peak, or rate of current decay (Fig. 7). These tests indicate that voltage control was achieved rapidly enough in all of the cells included in the present study, to ensure minimal distortion in measurements of current magnitude and inactivation parameters. In contrast, activation of I_{Na} at some potentials was so rapid that it was certainly distorted by the capacitive charging current.

TTX Sensitivity

From our results with small numbers of cells from each age tested for TTX response (Fig. 10), we estimate that $K_{0.5}$ for toxin block of I_{Na} is less than 1 nM, and does not change substantially throughout the first week of development. Our purpose here was not to try to distinguish fine differences in TTX sensitivity among the various ages. This would have required much larger samples, and complete dose sequences on each cell.

Previous studies suggested that the heart was unresponsive to TTX at early stages, and that sensitivity increased with development (reviewed in DeHaan, 1980). In these investigations, sensitivity was defined as the concentration of toxin required to cause cessation of spontaneous beating, or the number of preparations that stopped beating at a given concentration. However, when $\dot{V}_{max}$ was used to assess TTX effect, results similar to those reported here were found, showing that TTX sensitivity of chick ventricle remained constant throughout development (Iijima & Pappano, 1979; Marcus & Fozzard, 1981). From microelectrode measurements, Marcus and Fozzard (1981) reported that TTX reduced the $\dot{V}_{max}$ of the AP at all stages studied, from 3.5d (stage 21) to 18d of development and in the adult, with a half-effective concentration of about 10 nM. The discrepancy in $K_{0.5}$ between their results and ours can be explained by the nonlinear relation known to exist between $\dot{V}_{max}$ and G_{Na} (Cohen et al., 1984).

Two kinds of sodium channels can be distinguished in various excitable cells, on the basis of their functional properties and binding strength for TTX and STX (Rogart, 1986; Weiss & Horn, 1986). In excised patches of 11d chick ventricle cell membrane, Ten Eick et al. (1984) found that 3 nM TTX blocked a larger fraction of rapidly opening channels than those whose openings were delayed, whereas at 300 nM the toxin blocked all currents. These workers concluded that chick cells contain two classes of channels, those with high TTX affinity and short latencies, and a smaller low-affinity group with more delayed openings. In "myoballs" prepared from embryonic rat skeletal muscle myoblasts, the fast sodium current was carried by both high-affinity (K_D = 13 nM) and low-affinity (K_D = 3.2 μM) channels functioning in parallel, the low-affinity type accounting for about two-thirds of the current density (Gonoi, Sherman & Catterall, 1985). As myoblasts fuse into myotubes and mature, the proportion of high-affinity channels increases (Weiss & Horn, 1986). The experiments reported here indicate that effectively all of the fast sodium current was blocked by nanomolar TTX (Fig. 9). This indicates that no appreciable fraction of low-affinity channels with slow kinetics exists in chick embryonic ventricle cells under the conditions used here, in contrast to those reported in nerve (Sigworth, 1981), frog muscle (Patlak & Ortiz, 1986) and mammalian heart (Brown et al., 1982; Patlak & Ortiz, 1985; Follmer et al., 1987).

Role of I_{Na} in the Embryonic Action Potential

During development of numerous excitable cells, the AP upstroke shifts gradually from dependence on Ca to Na (DeHaan, 1980; Spitzer, 1981) as the sodium conductance increases. Despite the evidence presented here for an appreciable sodium current in 2d chick heart cells, the main depolarizing current underlying the cardiac AP at that time appears to be I_{Ca} (Galper & Catterall, 1978; DeHaan, 1980). Cardiac tissue from 2d embryos generates slowly rising action potentials (5 to 10 V/sec), which continue after exposure to TTX or Na-free bathing solution (Sakai et al., 1983). However, these AP's are reduced in amplitude by a decrease in extracellular Ca. We have recently measured a rapidly inactivating Ca current of about 6 μA/cm^2,

adequate to account for the slow AP upstroke velocity in 2d embryonic chick ventricle cells (Fujii et al., 1986*b*). In the 3d heart, also, the AP is not blocked by TTX or Na-free solution (Ishima, 1968), and beating is suppressed by calcium-channel blockers such as verapamil derivatives or manganese (Galper & Catterall, 1978). Nonetheless, cells from 3d hearts contain binding sites for radioactively labeled TTX (Lombet et al., 1981), and they respond to sea anemone toxin with an increase in AP upstroke velocity and a prolongation of the AP plateau (Lazdunski et al., 1982) that are characteristic of an inactivation-blocked I_{Na}. The results reported here confirm previous evidence (Fujii et al., 1986*a*) that I_{Na} is already present in cells of the 2d ventricle. The fact that this current makes no contribution to the spontaneous AP at this stage is readily explained by the low maximal diastolic potential which is about −60 mV. From the steady-state inactivation curve obtained here (Fig. 8) or that reported by Ebihara and Johnson (1980), it is apparent that the available sodium current in the 2d cell would be held in a state of perpetual inactivation. Between 2d and 7d, two developments account for the increase in AP upstroke velocity: the growth in number of I_{Na} channels, described in the present study; and the negative shift of maximal diastolic potential with development. In 3d heart cells, diastolic potential was −62 mV (McDonald & DeHaan, 1973), while the AP started from −90 mV in 7d ventricle cells (DeHaan, 1980; Veenstra & DeHaan, 1986).

Conclusions

1. The excitatory sodium current (I_{Na}) is present in ventricle cells taken from chick embryos after two, three, four and seven days of development. 2. At the earliest stage (2d + 6–8h, stage 12) the current density is small (28 μA/cm^2) and has slow inactivation kinetics (τ_h = 2 msec). 3. Between 2d and 7d of development, I_{Na} current density increases eightfold, and τ_h decreases from 2 to 1 msec. 4. Other characteristics of the current: activation kinetics, voltage dependence, and high TTX-sensitivity, show no statistically significant changes with development. 5. The Ca-dependence of the AP upstroke on the second day of development results from the relatively depolarized level of the diastolic potential, and failure to activate the available excitatory Na current. The shift from Ca to Na dependence during the third to the seventh day of incubation results partly from the increasingly negative diastolic potential and partly from the increase in available Na conductance.

We thank B. Duke Cuti for preparation of the cell cultures and W. Scherer for processing the manuscript. R. Penrod was especially generous with technical assistance and data analysis. The programmable digital signal generator and data processing programs were designed by W. N. Goolsby. This work was supported by NIH grant P01-HL 27385 to RLD.

References

Ayer, R.K., Jr., Fujii, S., DeHaan, R.L. 1985. A negative voltage shift in sodium current inactivation in embryonic heart cells caused by bath flow. *Biophys. J.* **47**:436a

Beeler, G.W., Reuter, H. 1970. Voltage clamp experiments on ventricular myocardial fibres. *J. Physiol. (London)* **207**:165–190

Bekkers, J.M., Greeff, N.G., Keynes, R.D. 1986. The conductance and density of sodium channels in the cut-open squid giant axon. *J. Pysiol. (London)* **377**:463–486

Brown, A.M., Lee, K.S., Powell, T. 1981. Sodium current in single rat heart muscle cells. *J. Physiol. (London)* **318**:479–500

Bustamente, J.O., McDonald, T.F. 1983. Sodium currents in segments of human heart cells. *Science* **220**:320–321

Cachelin, A.B., Peyer, J.E. de, Kokubun, S., Reuter, H. 1983. Sodium channels in cultured cardiac cells. *J. Physiol. (London)* **340**:389–401

Campbell, D.T., Hahin, R. 1984. Altered sodium and gating current kinetics in frog skeletal muscle caused by low external pH. *J. Gen. Physiol.* **84**:771–788

Clay, J.R., DeFelice, L.J., DeHaan, R.L. 1979. Current noise parameters derived from voltage noise and impedance in embryonic heart cell aggregates. *Biophys. J.* **28**:169–184

Cohen, C.J., Bean, B.P., Tsien, R.W. 1984. Maximal upstroke velocity as an index of available sodium conductance. Comparison of maximal upstroke velocity and voltage clamp measurements of sodium currents in rabbit Purkinje fibers. *Circ. Res.* **54**:636–651

Colatsky, T.J. 1980. Voltage clamp measurements of sodium channel properties in rabbit cardiac Purkinje fibers. *J. Physiol. (London)* **305**:215–234

Corey, D.P., Stevens, C.F. 1983. Science and technology of patch-recording electrodes. *In:* Single Channel Recording. B. Sakmann and E. Neher, editors. pp. 53–68. Plenum, New York

Courad, F., Martin-Moutot, N., Koulakoff, A., Berwald-Netter, Y. 1986. Neurotoxin-sensitive sodium channels in neurons developing in vivo and in vitro. *J. Neurosci.* **6**:192–198

DeHaan, R.L. 1980. Differentiation of excitable membranes. *Curr. Top. Dev. Biol.* **16**:117–164

DeHaan, R.L., McDonald, T.F., Sachs, H.F 1975. Development of tetrodotoxin sensitivity of embryonic chick heart cells in vitro. *In:* Developmental and Physiological Correlates of Cardiac Muscle. M. Lieberman and T. Sano, editors. pp. 155–167. Raven, New York

Doyle, D.D., Brill, D.M., Wasserstrom, J.A., Karrison, T., Page, E. 1985. Saxitoxin binding and "fast" sodium channel inhibition in sheep heart plasma membrane. *Am. J. Physiol.* **249**:H328–H336

Draper, M.H., Weidmann, S. 1951. Cardiac resting and action potentials recorded with an intracellular electrode. *J. Physiol. (London)* **115**:74–94

Ebihara, L., Johnson, E.A. 1980. Fast sodium current in cardiac muscle. *Biophys. J.* **32**:779–790

Ebihara, L., Shigeto, N., Lieberman, M., Johnson, E.A. 1980. The initial inward current in spherical clusters of chick embryonic heart cells. *J. Gen. Physiol.* **75**:437–456

Fenwick, E.M., Marty, A., Neher, E. 1982. Sodium and calcium channels in bovine chromaffin cells. *J. Physiol. (London)* **331**:598–635

Fernandez, J.M., Fox, A.P., Krasne, S. 1984. Membrane patches and whole cell membranes: A comparison of electrical properties in rat clonal pituitary (GH3) cells. *J. Physiol. (London)* **356**:565–585

Follmer, C.H., Ten Eick, R.E., Zeh, J.Y. 1987. Sodium current kinetics in cat atrial myocytes. *J. Physiol. (London)* **384**:169–187

Fozzard, H.A., January, C.T., Makielski, J.C. 1985. New studies of the excitatory sodium current in heart muscle. *Circ. Res.* **56**:475–485

Fujii, S., Ayer, R.K., Jr., DeHaan, R.L. 1986*a*. Differentiation of transmembrane ionic currents in the early embryonic chick heart. *In:* Progress in Developmental Biology, Part A. H.C. Slavkin, editor. pp. 353–356. Alan R. Liss, New York

Fujii, S., Ayer, R.K., Jr., Penrod, R., DeHaan, R.L. 1986*b*. Calcium current in heart cells isolated from 2-day and 7-day chick embryos. *Proc. XXXth Cong. Int. Union Physiol. Sci. (Tokyo)* 560a

Fujii, S., Hirota, A., Kamino, K. 1981. Optical recording of development of electrical activity in embryonic chick heart during early phases of cardiogenesis. *J. Physiol. (London)* **311**:147–160

Galper, J.B., Catterall, W.A. 1978. Developmental changes in the sensitivity of embryonic heart cells to tetrodotoxin and D600. *Dev. Biol.* **65**:216–227

Gonoi, T., Sherman, S.J., Catterall, W.A. 1985. Voltage clamp analysis of tetrodotoxin-sensitive and -insensitive sodium channels in rat muscle cells developing in vitro. *J. Neurosci.* **5**:2559–2564

Hahin, R., Campbell, D.T. 1983. Simple shifts in the voltage dependence of sodium channel gating caused by divalent cations. *J. Gen. Physiol.* **82**:785–805

Hodgkin, A.L., Huxley, A.F. 1952. The dual effect of membrane potential on sodium conductance in the giant axon of *Loligo*. *J. Physiol. (London)* **116**:497–506

Iijima, T., Pappano, A.J. 1979. Ontogenetic increase of the maximal rate of rise of the chick embryonic heart action potential. Relationship to voltage, time and tetrodotoxin. *Circ. Res.* **44**:358–367

Ishima, Y. 1968. The effect of tetrodotoxin and sodium substitution on the action potential in the course of development of the embryonic chick heart. *Proc. Jpn. Acad.* **44**:170–175

Keller, B.U., Hartshorne, R.P., Talvenheimo, J.A., Catterall, W.A., Montal, M. 1986. Sodium channels in planar lipid bilayers: Channel gating kinetics of purified sodium channels modified by batrachotoxin. *J. Gen. Physiol.* **88**:1–23

Kunze, D.L., Lacerda, A.E., Wilson, D.L., Brown, A.M. 1985. Cardiac sodium currents and the inactivating, reopening and waiting properties of single cardiac sodium channels. *J. Gen. Physiol.* **86**:691–719

Lazdunski, M., Renaud, J.F., Romey, S., Fosset, M., Barhanin, J., Lombet, A. 1982. Properties of the fast sodium channel and of the muscarinic receptor during development of embryonic heart cells in ovo and in vitro: *In:* Cardiac Rate and Rhythm. L.N. Boumann and H.J. Jongsma, editors. pp. 605–629. Martinus Nijhoff, The Hague

Lombet, A., Kazazoglou, T., Delpont, E. Renaud, J.F., Lazdunski, M. 1983. Ontogenic appearance of Na^+ channels characterized as high affinity binding sites for tetrodotoxin during development of the rat nervous and skeletal muscle systems. *Biochem. Biophys. Res. Commun.* **110**:894–901

Lombet, A., Renaud, J.F., Chicheportiche, R., Lazdunski, M. 1981. A cardiac tetrodotoxin-binding component: Biochemical identification, characterization and properties. *Biochemistry* **20**:1279–1285

McDonald, T.F., DeHaan, R.L. 1973. Ion levels and membrane potential in chick heart tissue and cultured cells. *J. Gen., Physiol.* **61**:89–109

McDonald, T.F., Sachs, H.G., DeHaan, R.L. 1972. Development of sensitivity to tetrodotoxin in beating chick embryo hearts, single cells, and aggregates. *Science* **176**:1248–1250

Makielski, J.C., Sheets, M.F., Hanck, D.A., January, C.T., Fozzard, H.A. 1987. Sodium current in voltage clamped internally perfused canine cardiac Purkinje cells. *Biophys. J.* **52**:1–11

Manasek, F.J. 1970. Histogenesis of the embryonic myocardium. *Am. J. Cardiol.* **25**:149–168

Marcus, N.C., Fozzard, H. 1981. Tetrodotoxin sensitivity in the developing and adult chick heart. *J. Mol. Cell. Cardiol.* **13**:335–340

Mazzanti, M., DeFelice, L.J. 1987. Na channel kinetics during the spontaneous heart beat in embryonic chick ventricle cells. *Biophys. J.* **52**:95–100

Nathan, R.D., DeHaan, R.L. 1978. In vitro differentiation of a fast Na^+ conductance in embryonic heart cell aggregates. *Proc. Natl. Acad. Sci. USA* **75**:2776–2780

Nathan, R.D., DeHaan, R.L. 1979. Voltage clamp analysis of embryonic heart cell aggregates. *J. Gen. Physiol.* **73**:175–198

Nathan, R.D., Pooler, J.P., DeHaan, R.L. 1976. Ultraviolet-induced alterations of beat rate and electrical properties of embryonic chick heart cell aggregates. *J. Gen. Physiol.* **67**:27–44

Noda, M., Ikeda, T., Kayano, T., Suzuki, H., Takeshima, H., Kurasaki, M., Takahashi, H., Numa, S. 1986. Existence of distinct sodium channel messenger RNAs in rat brain. *Nature (London)* **320**:188–192

Noda, M., Shimizu, S., Tanabe, T., Takai, T., Kayano, T, Ikeda, T., Takahashi, H., Nakayama, H., Kanaoka, Y., Minamino, N., Kanagawa, K., Matsuo, H., Raftery, R.A., Hirose, T., Inayama, S., Hayashida, H., Miyata, T., Numa, S. 1984. Primary structure of *Electrophorus electricus* sodium channel deduced from cDNA sequence. *Nature (London)* **312**:121–127

Patlak, J.B., Ortiz, M. 1985. Slow currents through single sodium channels of the adult rat heart. *J. Gen. Physiol.* **86**:89–104

Patlak, J.B., Ortiz, M. 1986. Two modes of gating during late Na^+ channel currents in frog sartorius muscle. *J. Gen. Physiol.* **87**:305–326

Reuter, H. 1984. Ion channels in cardiac cell membranes. *Annu. Rev. Physiol.* **46**:473–474

Rogart, R.B. 1986. High-STX-affinity vs. low-STX-affinity Na^+ channel subtypes in nerve, heart, and skeletal muscle. *Ann. N.Y. Acad. Sci.* **479**:402–430

Sakai, T., Fujii, S., Hirota, A., Kamino, K. 1983. Optical evidence for calcium-action potentials in early embryonic precontractile chich heat using potential-sensitive dye. *J. Membrane Biol.* **72**:205–212

Sakmann, B., Neher, E. 1984. Patch clamp techniques for studying ionic channels in excitable membranes. *Annu. Rev. Physiol.* **46**:455–472

Schmidt, J.W., Catterall, W.A. 1986. Biosynthesis and processing of the alpha subunit of the voltage-sensitive sodium channel in rat brain neurons. *Cell* **46**:437–445

Shigenobu, K., Sperelakis, N. 1971. Development of sensitivity to tetrodotoxin of chick embryonic hearts with age. *J. Mol. Cell. Cardiol.* **3**:271–286

Sigel, E. 1987. Properties of single sodium channels translated by *Xenopus* oocytes after injection with messenger ribonucleic acid. *J. Physiol. (London)* **386**:73–90

Sigworth, F.J. 1981. Covariance of nonstationary sodium current fluctuations at the node Ranvier. *Biophys. J.* **34**:111–133

Sperelakis, N., Shigenobu, K. 1972. Changes in membrane properties of chick embryonic hearts during development. *J. Gen. Physiol.* **60**:430–453

Spitzer, N. 1981. Development of membrane properties in vertebrates. *Trends Neurosci.* **4**:169–171

Ten Eick, R., Yeh, J., Matsuki, N. 1984. Two types of voltage dependent Na channels suggested by differential sensitivity of single channels to TTX. *Biophys. J.* **45**:70–73

Veenstra, R.D., DeHaan, R.L. 1986. Electrotonic interactions between aggregates of chick embryo cardiac pacemaker cells. *Am. J. Physiol.* **250**:H453–H463

Weiss, R.E., Horn, R. 1986. Functional differences between two classes of sodium channels in developing rat skeletal muscle. *Science* **233**:361–364

Received 6 August 1987; revised 18 November 1987